Journal of Theoretical and Applied Mechanics, Sofia, Vol.53 (2023) pp. 66-81
FLUID MECHANICS

IMPACT OF VARIABLE PASSAGE SECTION AND ZIGZAG ABSORBER ON THE THERMAL PERFORMANCE OF A THERMO-SOLAR CONVERTER FOR DRYING

FETHI MOUSSA BOUDJEMA[1], HAMIDOU BENZENINE[1,2*]

[1]*Smart Structures Laboratory, Faculty of Science and Technology, University Belhadj Bouchaib BP 284, Ain Témouchent, 46000, Algeria*
[2]*Laboratory of Energetic and Applied Thermal (ETAP), Faculty of Technology, B.P 230, University of Tlemcen, 13000, Algeria*

[Received: 16 October 2021. Accepted: 17 October 2022]

doi: https://doi.org/10.55787/jtams.23.53.1.66

ABSTRACT: This paper presents a numerical study of a two-dimensional laminar airflow transferred in a thermo-solar collector with forced convection. Simulations were processed to determine and analyze the dynamic and thermal fields under the influence of variation of collector configuration. Two cases of collector geometry (model of narrowing at exit and model of widening at entry) were studied and compared to the simple case uniform solar collector based on variations in temperature and velocity at the collector outlet for an input velocity varying between 0.04 and 0.11 m/s. The results show that the collector equipped with a zigzag-shaped absorber with a narrowing of the section at the outlet or widening at the inlet contribute to the thermal and dynamic improvement of the flow in the air stream compared with a simple case. The best performing case is recorded for the narrowest case of the exit shrinkage model where the exit velocity has been increased by 250%. this velocity reduces the drying time and increases the efficiency of the evacuation of the humid air leaving the chamber.

KEY WORDS: solar collector, zigzag absorber, humid air, efficiency, CFD.

1 INTRODUCTION

Solar radiation is a renewable energy resource that can be used to dry food products directly or indirectly. The solar collector for drying is a system that converts solar energy into thermal energy. The improvement of its thermal and dynamic performances has been the objective of several researchers. New forms of collector exchange surface have been proposed to increase the heat flux absorbed by the air. Others consider

*Corresponding author e-mail: hamidou.benzenine@univ-temouchent.edu.dz

that the improvement can be increased by incorporating baffles of different sizes, positions, and orientations. Ahmed-Zad et al. [1] studied how to improve the efficiency of the solar dryer by introducing baffles of different shapes: longitudinally shaped delta baffles, longitudinally bent ogival baffles, and longitudinal, transverse baffles. The results indicate that baffles in the dynamic flow path of a solar plate collector increase the heat transfer and the temperature at the outlet.

Ben Slama [2] also performed experimental work on the airflow behavior and heat transfer characteristics in an indirect solar dryer collector. The collector contains two air ducts: the first one is between the glazing and the absorber, and the second is between the absorber and the insulation, which have mixed transverse or longitudinal baffles. Fevzi Gulcimen et al. [3] reported that the flat galvanized absorber equipped with inclined fins with three angles (30°, 45°, and 60°) with forced convection reduces the time to 7 h instead of 22 h for free convection drying. Solar collectors often use single, porous or corrugated absorbers with a reference collector geometry. In this context, Wei and Man [4] numerically analyzed the airflow in an indirect natural convection solar dryer containing a porous absorber. The researchers concluded that using an inclined porous absorber increases the temperature and air velocity at the outlet.

Abhay et al. [5] experimentally studied an indirect solar dryer for drying bananas. The dryer consists of a solar collector equipped with a zigzag absorber with a total area of 2 m^2, an insulated drying chamber, and a chimney for air exhaust. The authors found that this drying type is faster and more efficient than natural air drying and noted that drying with a zigzag absorber is faster and more efficient than a flat absorber. The average thermal efficiency of the collector was 31.5%, and that of the drying chamber was 22.38%. Abhay et al. [6] also presented a numerical study based on the experimental data of a solar dryer. The researchers studied the effect of changing the height and angle of the V-shaped corrugation of the collector absorber. The results indicate that changing the corrugation shape promotes the heat transfer velocity from 0.58 to 0.73 m/s. Thus, it increases the system's thermal efficiency by 64.5% for a height of 1 cm and an angle of 20°.

Experimental work was carried out by Khalil [7] on an indirect solar dryer with forced convection. The dryer had two corrugated V-shaped absorption solar air collectors with two air passages to dry two agricultural products: apricots and grapes. The results show that apricots and grapes are dried at 60°C and 65°C, respectively, with an air velocity of 0.3 m/s. Satyender [8] conducted a two-pass solar collector's experimental and numerical study. The researcher introduced a porous serpentine corrugated bed on the absorber plate to increase the heat transfer. The results were compared with a single-pass solar collector. A considerable improvement in thermal efficiency at the two-pass collector was noted. The efficiency reached 80% at a flow

rate of 0.03 kg/s. This efficiency is much higher than that of a single-pass collector, whose efficiency varies between 56% and 62%.

Ksavan et al. [9] carried out an experimental study of potato drying in an indirect solar dryer. The triple-pass air collector uses sand for thermal storage. This dryer can reduce the moisture content from 79.1% to 9.1% of the dry matter in a drying period of 4.5 hours. The authors found that this type of collector is more efficient and can give an outlet temperature of 62°C at a flow rate of 0.062 kg/s. Therefore, significant improvements in thermal efficiency of up to 53.57%. Dilip Jain [10] analyzed a solar dryer equipped with a multi-pass inclined plane solar collector with thermal storage. The results show that increasing the length and width of the collector increases the absorbing surface and storage capacity, resulting in better drying performance. In 2007, Jain [11] developed a new type of natural convection dryer with thermal storage material to ensure heat air during the non-sunny period. Mohanraj [12] proposed an indirect dryer with forced convection to dry chili under metrological conditions in Pollachi, India. The collector contains sand mixed with aluminum scrap for thermal storage.

Fahmi [13] investigated dual-pass air-cooled solar thermal collectors with a porous layer of volcanic rock used as a thermal storage material undergoing solar drying. In addition, the author developed a mathematical model based on energy balance equations. The optimal efficiencies obtained for the intensities of 500 W/m^2 and 800 W/m^2 were 62% to 64%, respectively, with a flow rate of 0.035 kg/s. Bennamoun et al. [14] presented an experimental study to show the importance of solar drying using additional heating compared to non-additional drying; the authors concluded that heating the air at the collector inlet helps accelerate the drying time. Chouicha [15] also studied hybrid solar drying of potatoes sliced by forced convection using additional energy through Joule heating generated by photovoltaic modules connected in parallel.

Benzenine et al. [16] conducted a numerical analysis of two-dimensional laminar airflow passing through a solar collector provided with three length shoulder. The results show that using a shoulder placed on the insulator or the absorber contributes to increasing the dynamic and thermal performances of the flow compared to the simple case. Bhattacharyya et al. [17] analyzed the heat transfer in a solar air collector fitted with rectangular-shaped fins. The effects of the number and size of the fins have been studied. The authors noticed that the temperature of the fluid at the outlet increases with raise in the number of fins and decreases when it exceeds 80 fins. Daliran et al. [18] carried out experimental and theoretical work of a flat plate air collector. The study of the thermal performance of this system was carried out by comparing two models (without fin and with rectangular fin). The researchers reported that integrating the fins in the air channel creates a turbulent airflow and reduces the Nusselt number.

Youcef-Ali [19] experimentally studied a solar collector with the insertion of thin rectangular plates oriented parallel to the flow and welded to the underside of the absorber. The author found that this method increases heat transfer and thermal performance. Imad [20] presented a series of numerical tests on a solar collector with two air passages. Curved perforated baffles were inserted in the absorber of this collector. After a comparative study of the different inclination angles of these baffles, the author chose the right configuration of 7°. It allowed obtaining the best efficiency, which reached 77% for an airflow of 0.03 kg/s. Moreover, the author concluded that the variation of the inclination angle of the perforated baffle reduces the pressure drop.

Several authors have reported that the change in the shape of the absorbent plates could improve the heat transfer from the solar collectors, which influences the performance of solar drying systems. Numerous thermal enhancement designs have been proposed and reviewed, but few studies have focused on a system to accelerate fluid flow. This technique is essential for proper air and humidity evacuation at the exit of the drying chamber.

This work introduces a new technique to improve laminar flow's dynamic and thermal performance in a flat-air solar collector equipped with a zigzag absorber. An inclined glass is added to ensure a cross-section narrowing at the collector exit or widening the cross-section at the entry. The influence of the height variation of these two models on the temperature and velocity variation at the collector exit is also studied. A comparison is made with the classical uniform case for a variable entry velocity.

2 Description of the System

Figure 1 illustrates the complete geometric configuration of the studied system. It is an indirect solar dryer to dry agri-food products (Fig. 1-a). This study investigates the dynamic and thermal performances of the "solar air collector" component, representing one of the dryer's main parts. To this end, we used the physical and geometrical characteristics of the planar solar air collector studied by Abhay Lingayat [5] (Fig. 1-b), namely:

- A glass cover with thickness $E = 0.004$ m.
- A black-painted copper absorber (Zigzag shape) with thermal conductivity $\lambda = 387.6$ W/mK.
- A rectangular box for the collector made from a galvanized iron frame $E = 5$ mm.
- A drying chamber of dimension ($1 \times 0.4 \times 1$ m) contains:

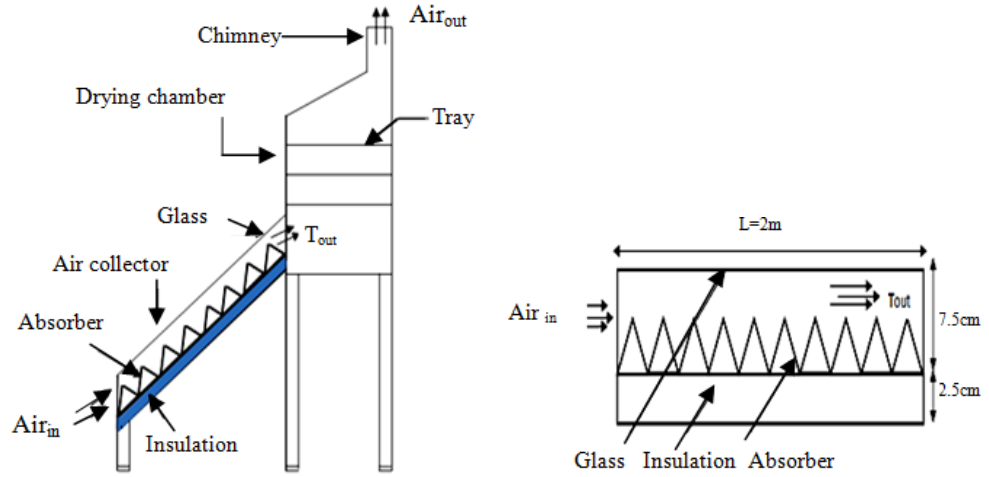

Fig. 1: Schematic representation of: (a) an indirect solar dryer; and (b) a solar air collector (thermo solar converter).

– Four aluminum trays stacked at a distance of 0.011 m.

– A chimney for the exhaust air at the height of 0.25 m.

Three different heights (H and h) (Table 1) between the glass and the absorber were varied at the input (H_i, $i = 1$ to 3) and at the output (h_i, $i = 1$ to 3) of the solar collector. We examined the impact of the widening of the passage section at the inlet (SW) and the narrowing of the section at the outlet (SN), respectively, and compared them with the case of a uniform section (SU).

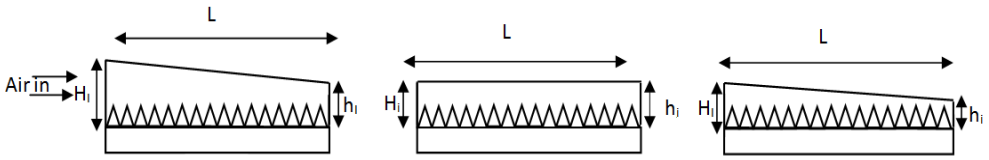

Fig. 2: Different models studied: (a) model of widening at entry SW; (b) model of uniform section SU; and (c) model of narrowing at exit SN.

Table 1: Dimensions of different collector models studied

Models	SU	SN			SW		
case	Case 01	Case 02	Case 03	Case 04	Case 05	Case 06	Case 07
H_i [cm]	7.5	7.5	7.5	7.5	8.5	9.5	10.5
h_i [cm]	7.5	6.5	5.5	4.5	7.5	7.5	7.5

3 Mathematical Modeling

3.1 Simplifying hypotheses

The following simplifying assumptions were adopted:

— The flow is assumed to be two-dimensional, stationary, and in a laminar regime.

— The fluid is assumed to be incompressible and Newtonian.

— The thermophysical properties of the fluid and solid are considered constant.

— The velocity and temperature profiles at the collector input are assumed to be constant and uniform.

3.2 Conservation equations

The equations governing the flow of air and heat transfer inside the flat solar collector were applied.

Continuity

$$\frac{\partial u}{\partial x} + \frac{\partial v}{\partial y} = 0\,. \tag{1}$$

Movement quantity equation

Next x

$$\rho\nu u\frac{\partial u}{\partial x} + v\frac{\partial u}{\partial y} = --\frac{1}{}\frac{\partial p}{\partial x} + \Big[\frac{\partial^2 u}{\partial x^2} + \frac{\partial^2 u}{\partial y^2}\Big]\,. \tag{2}$$

Next y

$$\rho\nu u\frac{\partial v}{\partial x} + v\frac{\partial v}{\partial y} = --\frac{1}{}\frac{\partial p}{\partial y} + \Big[\frac{\partial^2 v}{\partial x^2} + \frac{\partial^2 v}{\partial y^2}\Big]\,. \tag{3}$$

Energy equation

$$\rho C_p\Big(u\frac{\partial T}{\partial x} + v\frac{\partial T}{\partial y}\Big) = k\Big[\frac{\partial^2 T}{\partial x^2} + \frac{\partial^2 T}{\partial y^2}\Big], \tag{4}$$

where C_p is the specific heat and ρ is the air density.

3.3 Boundary conditions

The fluid flow field is required from boundary conditions in the proposed system.

1. *At the input collector*: The input velocity (U_{in}) varied between 0.04 and 0.11 m/s for all models to analyze the collector's thermal and dynamic behavior.

2. *At the output collector*: The pressure = Atmospheric pressure.

3. *At the lower wall (insulating)*: The adiabatic condition is applied.

4. *At the upper wall (glass)*: The absorption coefficient $\alpha = 0.05$.

5. *At the obstacle (absorber)*: Transmissivity coefficient $\tau = 0.9$. A uniform solar flux was imposed.

4 Numerical Results

4.1 Mesh sensitivity analysis

For different simulations carried out, an unstructured variable mesh with quadrilateral and triangular volumes, highly concentrated in the vicinity of the absorber, was used (Fig. 3).

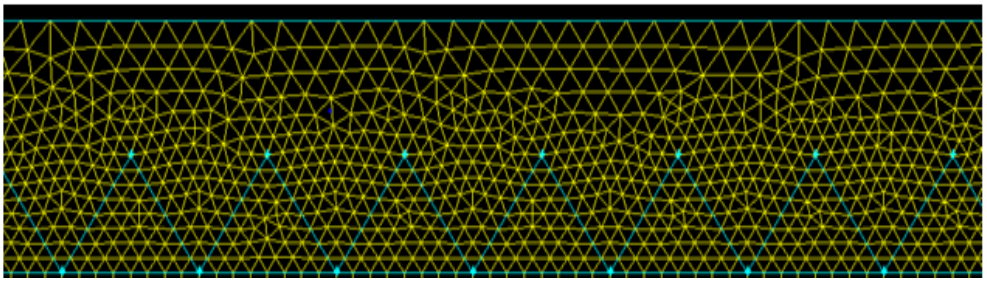

Fig. 3: Solar collector meshes with Gambit.

The study of the independence of the mesh is a very important phase in a computational fluid dynamics (CFD) analysis, given the influence of its parameters on the calculated solution of temperature and velocity at the output of the solar collector. For an input velocity(U_{in}) equal to 0.08 m/s, a series of tests on the five grids of the cell numbers 3056, 4310, 6966, 10984, and 16622 (Table 2) was performed. We note that the mesh grid with number 10984 gives a good compromise between the precision and mesh density.

Table 2: Mesh sensitivity test

Nodes	Cells	T_{out}	Absolute error T_{out}	U_{out}	Absolute error U_{out}
8-40	3056	332.4523	—	0.07723329	—
10-60	4310	333.8769	1.4246	0.08086187	0.00362858
12-100	6966	333.5573	0.3196	0.08641470	0.00555283
15-200	10984	333.5757	0.0184	0.08754016	0.00112546
20-250	16622	333.6432	0.0675	0.09399920	0.00645904

4.2 Model validation

Experimental data obtained by Abhay Lingayat et al. [5] was used to ensure the model validation used by the Fluent calculation code. Table 1 lists the parameters used in their experiments. Figure 4 illustrates the temperatures at the outlet of the collector (T_{out}) in the function of solar radiation.

The results obtained are in good agreement with the experimental work of Abhay Lingayat et al. [5]. Their results allowed us to study the proposed problem numerically.

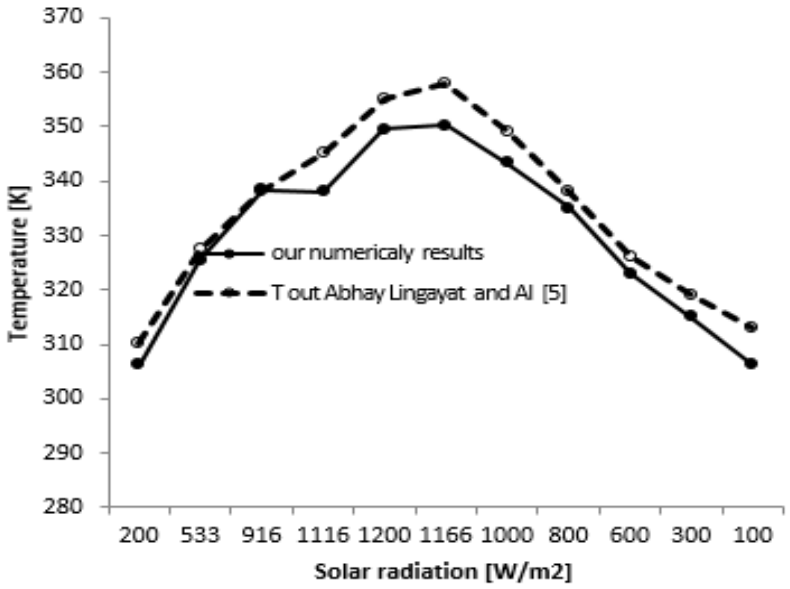

Fig. 4: Temperature at the outlet of the collector as a function of the solar radiation: comparison with Abhay Lingayat et al. [5].

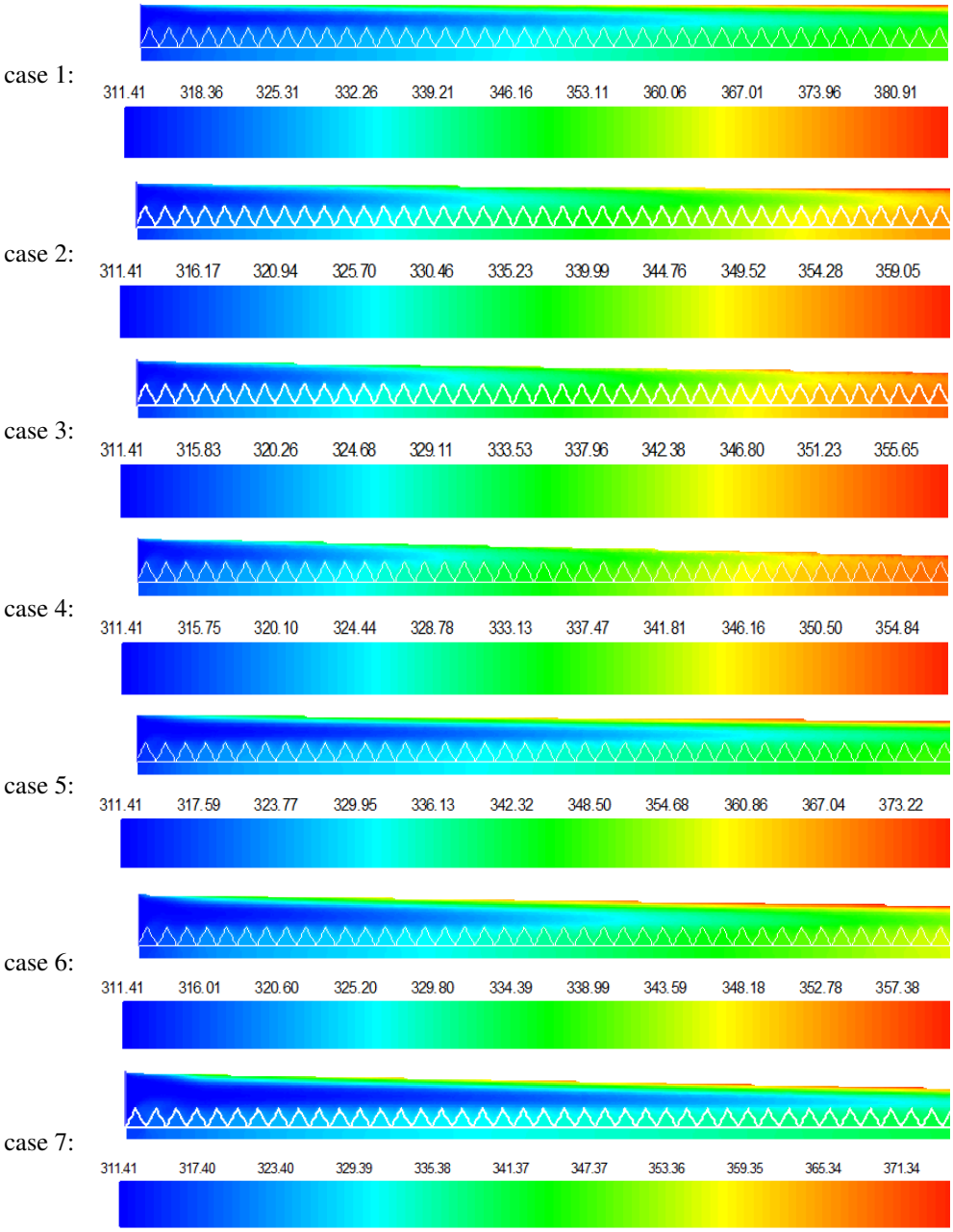

Fig. 5: Contours of the temperature obtained for different shapes at Input velocity $U_{\text{in}} = 0.04$ m/s.

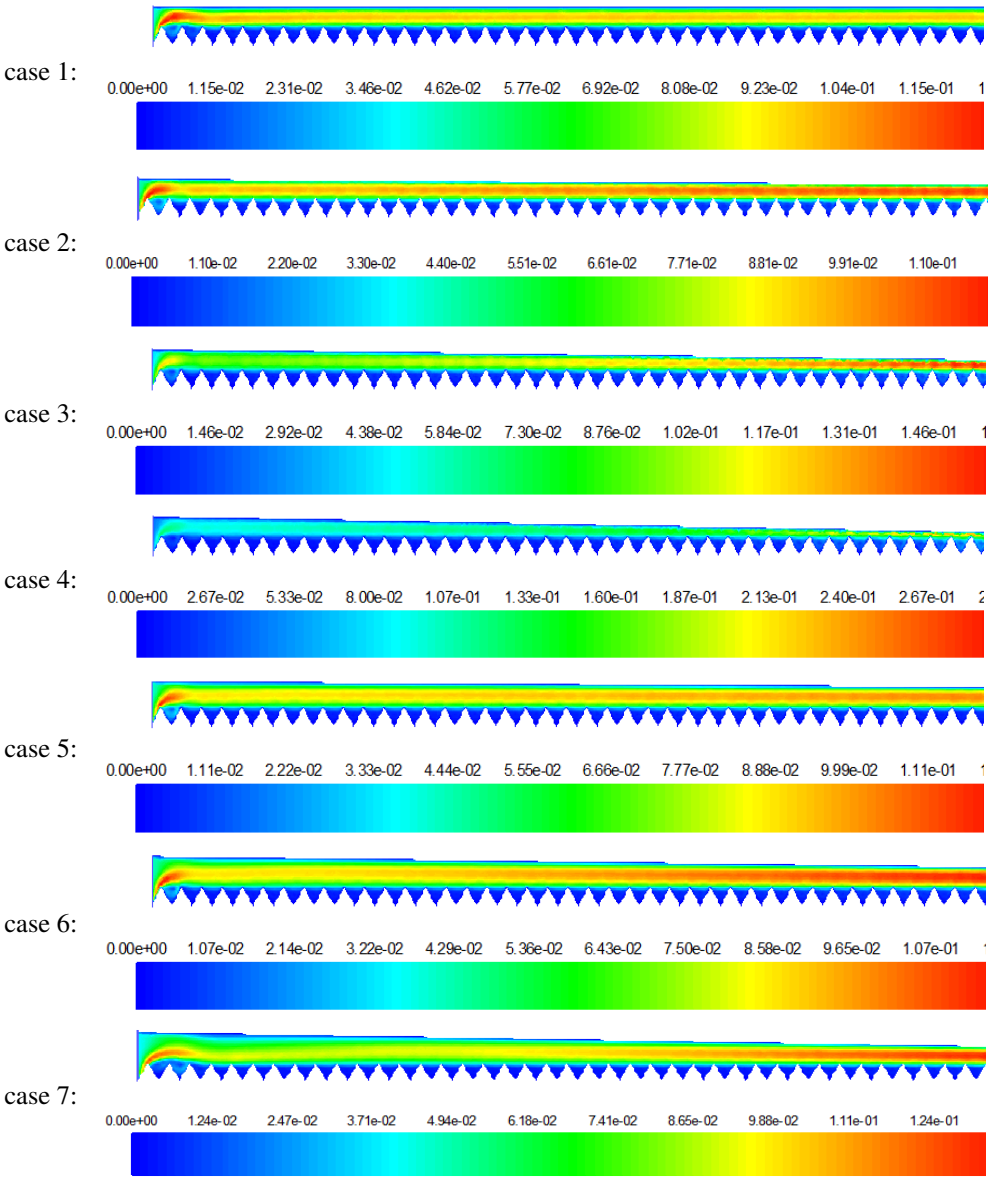

Fig. 6: Contours of velocity obtained for the different shapes, Input velocity = 0.04 m/s.

4.3 DYNAMIC AND THERMAL ASPECTS OF THE FLOW

Figures 4 and 5 show the contours of the temperature and the resulting velocity for an input velocity equal to 0.04 m/s for all the studied cases, respectively.

Figure 5 shows the air temperature field along the collector for the different configurations studied. The isothermal contours show that the temperature changes longitudinally in the dynamic vein of the solar collector. Low temperatures are observed at the entrance and gradually increase as we approach the exit. Using a zigzag-shaped absorber (V) increases the exchange surface and consequently improves the heat transfer within the fluid. The radiative heat flux received by this absorber is transported by the fluid in a more or less intense manner, depending on the case. The case of narrowing the passage section at the outlet SN (Cases 2, 3, and 4) significantly improves the transfer, compared to the case of widening the section at the entrance SW (Cases 5, 6, and 7). It should also be noted that the heat transfer intensification is proportional to the increase in the rate of narrowing or widening of the fluid section.

Figure 6 shows the contours of the resulting velocity for the simple case SU (Case 1) and for cases of narrowing SN (Cases 2, 3, and 4) and cases of enlargement SW (Cases 5, 6, and 7). It is clear that the maximum flow velocity is localized in the center of the channel and decreases more and more as we approach the two walls, which is obviously due to friction. These contours show that a zigzag-shaped absorber contributes to the generation of turbulence, which increases the mixing effect and, consequently, improves heat exchange.

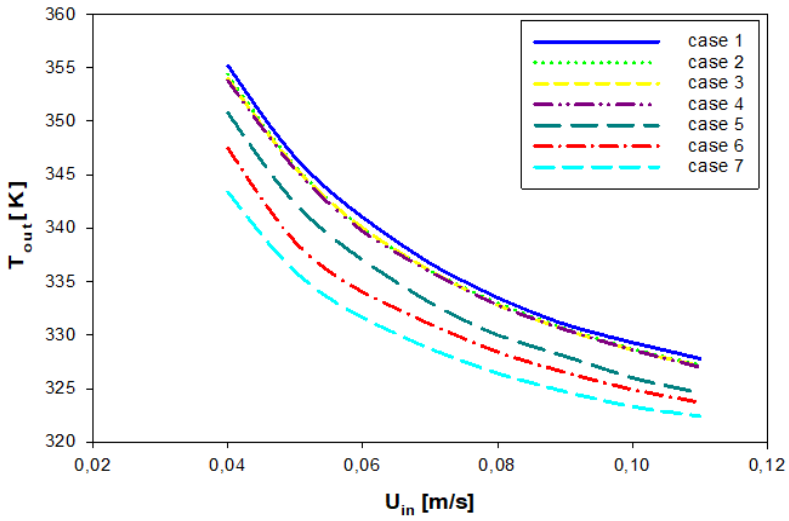

Fig. 7: Evolution of the temperature at the air collector outlet as a function of the input velocity for all cases.

The decrease in vein height leads to an increase in velocity, which can be seen in the second half of the channel by the red band (maximum velocity). This red band changes from one case to another depending on the height. By comparing the velocity contours obtained for the two cases (narrowing and widening) for different heights, we also note a similar flow behavior at both the channel's entry and exit, confirming the mass conservation principle.

Figure 7 shows the temperature evolution at the collector outlet (T_{out}) in the input velocity (U_{in}) interval studied for the cases of narrowing and widening at different heights compared with the simple case. It can be observed that the temperature values decrease with the increased input velocity for all configurations. Moreover, the simple case (SU) and the narrowing cases present the highest values compared to the widening case. Thus, the more the entry-exit section ratio (H/h) increases, the more the temperature at the exit becomes less important.

Figure 8 shows the variation of the average temperature calculated at cross-sections located at: $x = 0$ m (entry of collector), $x = 0.381$ m, $x = 0.761$ m, $x = 1.142$ m and at $x = 1.571$ m depending on all the cases studied for a chosen velocity ($U_{\text{in}} = 0.04$ m/s). Thus, it can be noted that the temperature profiles start with a reference temperature equal to 311 K at $x = 0$ m and increase as we approach the collector output. It should also be noted that the case of a uniform section and the narrow-

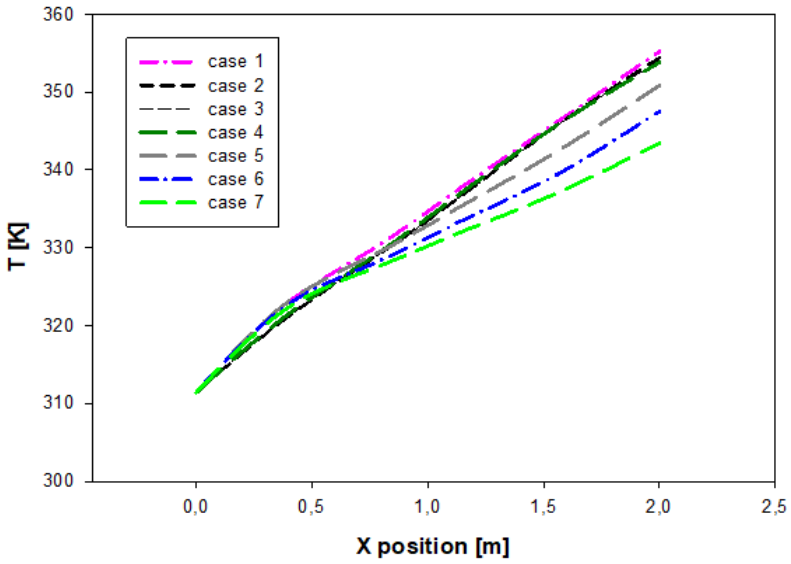

Fig. 8: Variation of the average temperature as a function of the distance of collector (x) for all cases.

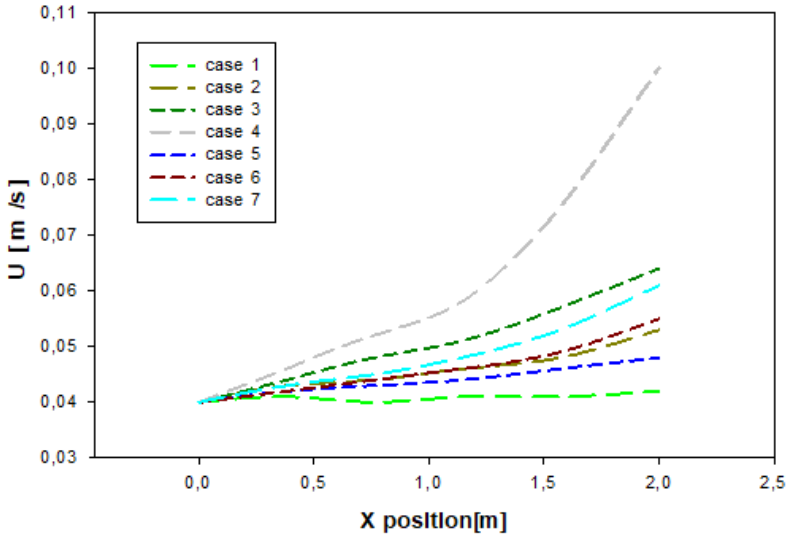

Fig. 9: Variation in the average velocity as a distance function for all cases.

ing cases have the highest average temperature values. At the same time, the lowest values are recorded for the widening cases.

Figure 9 shows the evolution of the average velocity calculated at selected sections at: $x = 0$ m, $x = 381$ m, $x = 0.761$ m, $x = 1.142$ m and $x = 1.571$ m according to

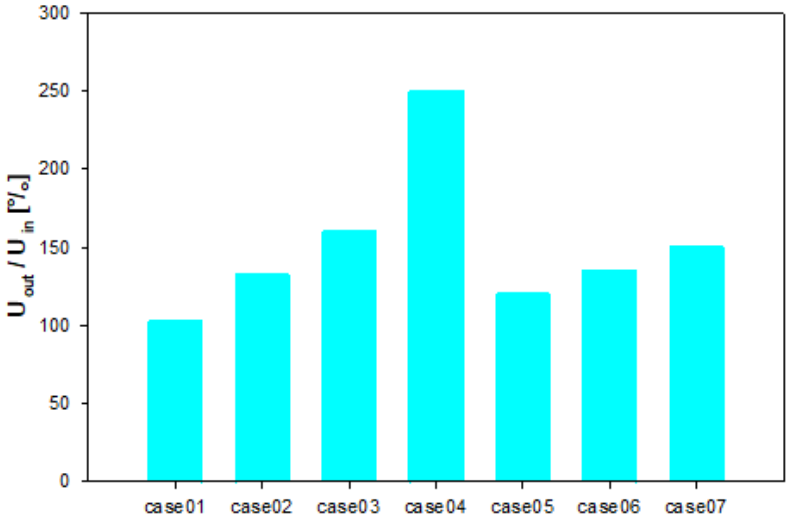

Fig. 10: Variation of the average temperature as a function of the distance of collector (x) for all cases.

the two models studied "widening and narrowing" at different section ratios and for a chosen flow rate inlet velocity ($U_{\text{in}} = 0.04$ m/s). The examination of these figures shows that the average velocity increases along the pipe for all cases. Also, in the case uniform section, the average velocity remains constant.

Figure 10 shows the collector output velocity ratio by input velocity 0.04 m/s for all the cases studied. The low ratio is observed for Case 1 (Sw), and the largest ratios are for those obtained for cases of SN narrowing and SW widening up to 2.5 times (250% in Case 4). The results explain the improvement of the dynamic performance in our study. Moreover, they show the impact of dynamic performance on improving air renewal in the drying chamber. Thus, they allow a better evacuation of the moist air and reduce the drying time.

5 Conclusions

In this work, Fluent's calculation code was used to simulate a numerical study of airflow's thermal and dynamic behavior by forced convection in a solar collector. The influence of the geometry of the collector input and output section was analyzed. The results show the temperature and velocity contours obtained for the models with different SN – SW cases. They were compared to the SU model for an input velocity interval between 0.04 and 0.11 m/s.

Furthermore, the results indicate that the intensification of heat transfer can be ensured by using the zigzag form of the absorber. The case of a uniform section SU and case SN have the highest average temperature values, whereas the lowest values are recorded for widening cases at the inlet SW. It should also be noted that the more the input-output section ratio (H/h) increases, the more the temperature at the outlet become has important.

Dynamically, the output velocity of the SW model in Case 4 was increased by 250% compared to the input velocity, which ensured a high flow rate at the entry of the drying chamber and thus a better evacuation of the moist air at the exit of the chimney. The results indicate that the zigzag shape of the absorber with the narrowing section at the exit of the collector or the widening at the entry is an effective system for accelerating and increasing the dynamic performance of the fluid flow through the solar collector. This technique is useful for a good evacuation of air and moisture released from the drying chamber.

References

[1] A. Ahmed-Zad, A. Moulla, S. Hantala, J.Y. Desmons (2001) Amélioration des Performances des Capteurs Solaires Plans Air: Application au Séchage de l'Oignon Jaune et du Hareng. *Rev. Energ. Ren.* 69-78.

[2] R. BEN SLAMA, M. COMBARNOUS (2011) Study of orange peels dryings kinetics and development of a solar dryer by forced convection. *Solar Energy* **85** 570-578.

[3] G. FEVZI, K. HAKAN, D. AYDIN (2016) Drying of sweet basil with solar air collectors. *Renewable Energy* **93** 77-86.

[4] C. WEI, Q. MAN (2014) Analysis of the heat transfer and airflow in solar chimney drying system with porous absorber. *Renewable Energy* **63** 511-518.

[5] A. LINGAYAT, V.P. CHANDRAMOHAN, V.R.K. RAJU (2016) Design, development and performance of indirect type solar dryer for banana drying. *Energy Procedia* **109** 409-416.

[6] A. LINGAYAT, V.P. CHANDRAMOHAN (2021) Numerical investigation on solar air collector and its practical application in the indirect solar dryer for banana chips drying with energy and exergy analysis. *Thermal Science and Engineering Progress* **26**(2) 101077.

[7] K.E.J. AL-JUAMILY, A.J.N. KHALIFA, T.A YASSEN (2007) Testing of the performance of a fruit and vegetable solar drying system in Iraq. *Desalination* **209** 163-170.

[8] S. SINGH (2020) Experimental and numerical investigations of a single and double pass porous serpentine wavy wiremesh packed bed solar air heater. *Renewable Energy* **145** 1361-1387.

[9] S. KESAVAN, T.V. ARJUNAN, S. VIJAYAN (2018) Thermodynamic analysis of a triple-pass solar dryer for drying potato slices. *Journal of Thermal Analysis and Calorimetry* **136** 159-171.

[10] J. DILIP (2005) Modeling the system performance of multi-tray crop drying using an inclined multi-pass solar air heater with in-built thermal storage. *Journal of Food Engineering* **71** 44-54.

[11] D. JAIN (2007) Modeling the performance of the reserved absorber w i th paked bed thermal storage natural convection solar crop dryer. *Journal of food engineering* **78** 637-647.

[12] M. MOHANRAJ P. CHANDRASEKAR (2009) Performance of a forced convection solar drier integrated with gravel as heat storage materiel for chili drying. *Journal of Engineering Science and Technology* **3** 305-314.

[13] A.F. ISMAIL, A.S.A. HAMID, A. IBRAHIM, H. JARIMI, K. SOPIAN (2022) Analysis of a double pass solar air thermal collector with porous media using lava rock. *Energies* **15**(3) 905.

[14] L. BENNAMOUN, A. BELHAMRI (2003) Design and simulation of a solar dryer for agriculture product. *Journal of Food Engineering* **59** 259-266.

[15] S. CHOUICHA, A. BOUBEKRI, D. MANOUCHE, M.H. BERRBEUH (2013) Solar drying of sliced potatoes an experimental investigation. *Energy Procedia* **36** 1276-1285.

[16] H. BENZNINE, B.S. ABBOUDI, R. SAIM (2020) Effect of the presence of a shoulder on the thermal and dynamic structure of a laminar flow in an air-plane solar collector. *Numerical heat transfer, Part B: Fubdamentals* **77**(3) 257-270.

[17] T. BHATTACHARYYAA, B. ANANDALAKSHMIB, K. SRINIVASANC (2017) Heat transfer analysis on finned plate Air Heating solar collector for its application in paddy drying. *Energy Procedia* **109** 353-360.

[18] A. DALIRAN, Y. AJABSHIRCHI (2018) Theoretical and experimental research on effect of fins attachment on operating parameters and thermal efficiency of solar air collector. *Information Processing in Agriculture* **5** 411-421.

[19] S. YOUCEF ALI (2005) Study and optimization of the thermal performances of the offset rectangular plate fin absorber plates with various glazing. *Renewable Energy* **30** 271-280.

[20] E.M.S. EL-SAID (2020) Numerical investigations of fluid flow and heat transfer characteristics in solar air collector with curved perforated baffles. *Engineering Reports* **2**(5).